Applied Catalysis B: Environmental 130–131 (2013) 84–92

Contents lists available at SciVerse ScienceDirect

Applied Catalysis B: Environmental

journal homepage: www.elsevier.com/locate/apcatb

Preparation of $Cu_2(OH)_3NO_3$/ZnO, a novel catalyst for methyl orange oxidation under ambient conditions

Assadawoot Srikhaow[a,b], Siwaporn Meejoo Smith[b,c,*]

[a] Materials Science and Engineering Graduate Program, Faculty of Science, Mahidol University, Rama VI Road, Rajathevi, Bangkok 10400, Thailand
[b] Center of Excellence for Innovation in Chemistry, Faculty of Science, Mahidol University, Rama VI Road, Rajathevi, Bangkok 10400, Thailand
[c] Department of Chemistry, Faculty of Science, Mahidol University, Rama VI Road, Rajathevi, Bangkok 10400, Thailand

ARTICLE INFO

Article history:
Received 4 May 2012
Received in revised form 1 September 2012
Accepted 16 October 2012
Available online 29 October 2012

Keywords:
Copper hydroxide nitrate
Zinc oxide
Layered hydroxyl salts
Catalytic wet oxidation
Wastewater treatment

ABSTRACT

This work reports a novel process to synthesize copper hydroxyl nitrate/zinc oxide composites ($Cu_2(OH)_3NO_3$/ZnO), and their application as a highly effective and reusable catalyst for wet oxidation of methyl orange (MO) under ambient conditions. No additional air or oxygen flow is required. Using a metal oxide assisted method, the $Cu_2(OH)_3NO_3$/ZnO composites were hydrothermally obtained by varying the Cu:Zn mole ratio (2:1, 4:1, and 6:1) and the structural, chemical and surface properties of the composites were investigated. Decolorization of 500 ppm MO can be effectively catalyzed by the $Cu_2(OH)_3NO_3$/ZnO composite (Cu:Zn = 4:1) with the color, chemical oxygen demand (COD) and total organic carbon (TOC) removal efficiencies being greater than 99%, 98% and 94%, respectively, after 20 min treatments using the catalyst loading of 3 g L^{-1}. Results from systematic catalytic activity tests strongly suggested that MO was oxidized by oxygen dissolved in the dye solution, and that the degradation pathway of MO possibly occurred through radical and H_2O_2 generation. The application of highly efficient $Cu_2(OH)_3NO_3$/ZnO catalysts in wastewater remediation may be attractive alternative to existing oxidation catalyst systems as they are low-cost, simple to prepare, feasible to operate under ambient conditions.

1. Introduction

Water pollution is one of the main environmental concerns impacting the world ecology. Therefore, water protection plans and wastewater treatments should receive a great attention as they impact the world's economic growth, global food production and industrial development. It is widely accepted that agricultural runoff and industrial wastewater may contain hazardous chemicals [1,2] and hence discharge of the polluted water without treatment can cause major damage to the quality of natural water reservoirs. Textile industries, in particular, intensively use chemicals (such as dyes and transfer reagents) and massive amounts of water in dyeing processes. Thus, significant amounts of dye contaminated effluent might be produced and effective treatment processes must be put in place to clean the water before releasing into waterways. One of the main research areas in wastewater treatment is developing a novel technology to effectively remove residual dyes and organic pollutants from wastewater [3–5]. Conventional methods used to remove pollutants from wastewater are adsorption, biological treatment and chemical oxidation [3,6]. Although adsorption is the simplest method, but less effective as pollutants were only transferred to the sorbent surface, and additional treatment of the contaminated solid is required [7]. Biological treatments are considered as promising alternatives. However, it may be rather difficult to biologically degrade some conjugated aromatic compounds due to their structural stability [8]. In addition, microorganisms may not be survived under extreme conditions (extreme pH or highly toxic) inhibiting effective biological treatments of wastewater [9,10].

Advanced oxidation processes (AOPs) have been described as chemical methods operated to induce the oxidative degradation of organic compounds by radical species [11,12]. Examples of AOPs include ozonation [13], Fenton process [14], photocatalysis [15], sonolysis [16] and other chemical oxidation processes induced by oxidizers such as air, O_2, O_3, and H_2O_2 [11,17,18]. To practically operate in industrial sites, the oxidation process should remove organic pollutants effectively under mild conditions, and with low cost. Photocatalytic oxidation and sonolysis are of interest as they can operate under ambient conditions with no requirement of additional oxidizer such as ozone and hydrogen peroxide [16,18]. However, industrial integration is difficult, as these require special maintenance/operation of high power light sources, or specialized sonication equipments. In recent years, a limited number of works have reported oxidation of organic compounds *via* catalytic

* Corresponding author at: Department of Chemistry, Faculty of Science, Mahidol University, Rama VI Road, Rajathevi, Bangkok 10400, Thailand. Tel.: +66 222015164; fax: +66 23547151.
E-mail addresses: siwaporn.smi@mahidol.ac.th, siwaporn.meejoo@gmail.com (S.M. Smith).

0926-3373/$ – see front matter © 2012 Elsevier B.V. All rights reserved.
http://dx.doi.org/10.1016/j.apcatb.2012.10.018

wet oxidation (CWO) at near ambient conditions, in which the organic substances undergo aerial oxidation over metal catalysts such as Fe_2O_3–CeO_2–TiO_2/γ-Al_2O_3 [19], MoO_3/Ce [20], polyoxomolybdate nanotubes [21], and ZnO/MoO_3 mixed oxide nanotubes [22]. Although no harmful chemical reagent is required, air or oxygen is necessary to activate these oxidation processes. Apart from the intrinsic properties of the catalyst, factors such as catalyst loading, concentration of the organic substrate, air flow rate (and, perhaps, its purity) can play significant roles in the efficiency and rate of the processes [5,12,23].

A few copper hydroxyl salts were reported as promising catalysts in azo dyes removal *via* catalytic wet peroxide oxidation (CWPO) in which H_2O_2 is required as oxidizer [24,25]. In 2010, Zhan and Chen reported the degradation of azo dyes over copper hydroxyphosphate, $Cu_2(OH)PO_4$, under near-neutral pH conditions [24], whereas copper hydroxide nitrate, $Cu_2(OH)_3NO_3$ is an effective CWPO catalyst for oxidative degradation of azo dyes in a wide pH range [25]. Previously reported, $Cu_2(OH)_3NO_3$ can be synthesized by several routes, such as precipitation of $Cu(NO_3)_2$ in a basic aqueous solution [26], urea hydrolysis of $Cu(NO_3)_2$ [27], chemical reaction between CuO and aqueous $Cu(NO_3)_2$ solution [28], cation exchange of Mg(II) for Cu(II) in aqueous $Cu(NO_3)_2$ solution and evaporation of aqueous $Cu(NO_3)_2$ solution [29].

To gain a significant advantage over the previously reported copper hydroxyl salt catalysts, an ideal catalyst should enable organic substrates to be oxidized under ambient conditions, with no requirement of additional continuously supplied oxidizing agent. In this work, $Cu_2(OH)_3NO_3$ (a copper hydroxyl salt) was incorporated with microcrystalline ZnO by a one-step hydrothermally metal oxide assisted method. This study also reports the application of this material (denoted as $Cu_2(OH)_3NO_3$/ZnO) as a highly effective and reusable catalyst for wet oxidation of methyl orange (MO) under ambient conditions without addition of oxidizer. Details on systematic investigations of the structural and catalytic activity of this material and possible degradation pathway of MO are discussed.

2. Experimental

2.1. Materials

All chemicals used in this work were commercially supplied as analytical grade reagents, and used without further purification. De-ionized water was used throughout the experiments. Copper nitrate trihydrate and copper sulphate pentahydrate were commercially obtained from Univar, while ZnO powdered material was obtain from Merck. Tert-butanol (Merck) and NaOH (Rankem) were employed as hydroxyl radical scavenger reagents.

2.2. Preparation method of flower-like ZnO

A D-glucose assisted precipitation method [30] was applied to obtain flower-like ZnO materials by using NaOH and $Zn(NO_3)_2$ (Qrëc) as starting reagents, a mixture of H_2O: acetone: ethyl acetate (3:3:2 by volume) as co-solvent, and D-glucose (Univar) as ion stabilizer. Obtained white precipitate was subsequently calcined at 400 °C for 3 h in an air atmosphere, giving a flower-like ZnO sample with S_{BET} = 11.7 m^2/g.

2.3. Preparation of the $Cu_2(OH)_3NO_3$/ZnO samples

A series of suspensions containing the flower-like ZnO (or commercial ZnO) powder in $Cu(NO_3)_2$ aqueous solutions were obtained by varying the Cu:Zn molar ratios (2:1, 4:1 and 6:1). Next, these suspensions were sonicated for 30 min in an ultrasonic bath, followed by a hydrothermal treatment at 100 °C in a 50 mL Teflon-lined stainless steel autoclave for 30 min. Subsequently, the reaction mixtures were left to stand at room temperature, allowing the suspensions to cool down. After filtering and washing with de-ionized water, the precipitates were freeze dried, and kept in a dry condition at room temperature.

2.4. Sample characterization

Structural properties of as-prepared samples were studied on a Bruker (AXS model D8 advance) powder X-ray diffractometer equipped with Cu K_α radiation, λ = 1.5419 Å, 2θ range = 5–50°, step = 0.050°, scan step = 1 s/step. FT-IR spectra were obtained on a Perkin Elmer (Spectrum GX FT-IR System) fourier-transform infrared spectrometer. The microstructure of catalyst samples was examined on a JEOL (JSM-6400) scanning electron microscope. Furthermore, energy dispersive X-ray (EDX) microanalyses were carried out to identify the chemical composition of catalyst samples. The surface properties were studied by using Brunauer–Emmett–Teller method (BET Model Quantachrome/Autosorb-1, Thermo Finnigan/Sorp-tomatic 1990). The concentration of elements in the samples was also determined on an X-ray fluorescence spectrometer (Bruker S4 EXPLORER) equipped operating in a He working mode (X-ray tube window = 75 μm; excitation = 4 kW) using a loose powder preparation method and a 34 mm sample cup.

2.5. Catalytic degradation experiments

All catalytic reactions were carried out using the same catalyst loading; 3 g L^{-1} of aqueous methyl orange (MO, 500 ppm) under stirring. The color removal efficiency of MO was monitored as a function of time by measuring absorbance of the dye solution after catalytic treatment at given time intervals. In order to terminate the reaction at specific reaction times, the catalyst was immediately filtered off using a Buchner funnel equipped with a water aspirator pump. UV–vis absorption spectra of the dye filtrates were recorded on a Perkin Elmer (Lamda 800) UV–vis spectrophotometer. Subsequently, the concentration of MO in the filtrates was quantified using the absorbance at 464 nm (corresponding to unreacted MO) and a curve fitting method using the Beer Lambert law. The color removal efficiency (η, %) of methyl orange was calculated by using this equation:

$$\eta(\%) = \frac{C_0 - C_t}{C_0} \times 100 \quad (1)$$

where C_0 is the initial concentration of MO and C_t is the concentration of MO after '*t*' min.

Total organic carbon (TOC) content in the dye solutions was determined by an in-house method (SGS laboratory service): LBEN-09149 based on United States Environmental Protection Agency, 2004, EPT method 9060A. Moreover, chemical oxygen demand (COD) was measured by a standard closed reflux/titration method [31]. The TOC removal efficiency is defined as:

$$\text{TOC removal efficiency } (\%) = \frac{TOC_0 - TOC_t}{TOC_0} \times 100 \quad (2)$$

where TOC_0 is initial TOC of the solution and TOC_t is TOC of solution after '*t*' min reaction time. Similarly, COD_0 and COD_t values were used instead of TOC_0 and TOC_t values in Eq. (2) respectively, to calculate COD removal efficiencies. The data from triplicate measurements were analyzed to obtain average values and standard deviation (SD). The significance of difference of data was evaluated using the Student's *T*-test and one-way ANOVA [32] at a significance level of 0.05.

To investigate the possible mechanism of decolorization of MO, the experiments were conducted under air atmosphere, vacuum in a closed system and in the presence of radical scavengers *i.e.* tert-butanol [33,34] and NaOH [35], into the solution at 25 °C. Detailed processes are described in the supplementary data.

The stability of catalyst, $Cu_2(OH)_3NO_3$/ZnO (Cu:Zn = 4:1) was studied by monitoring the generation of metal ions in the dye solution during catalytic wet oxidation. After 20-min reaction, the concentration of Cu and Zn ions in the dye filtrates was then determined by using a graphite furnace atomic absorption spectrometer (GFAAS, Perkin Elmer AAnalyst 100). A hollow cathode zinc lamp (Perkin Elmer) operated with 10-mA current was employed, with argon flow throughout the heating program, except during the atomization step.

2.6. Characterization of the degradation products

Liquid chromatography with ion trap mass analyzer (LC–MS, Agilent technology, Agilent 1100 equipped with Esquire 3000 plus) was employed to detect the degradation products upon the oxidation of methyl orange. The LC–MS system was equipped with C18 column and 30% of acetonitrile and 70% of 0.01 M ammonium acetate (pH 6.8) were used as a mobile phase. The flow rate used was 0.6 mL min^{-1}. The mass spectrometer was equipped with an electrospray ionization (ESI) source operating at negative polarity. This LC/MS system could detect mass ranged between 100 and 400 *m*/*z*.

3. Results and discussion

3.1. Characterization of the catalysts

Powder X-ray diffractograms of ZnO powder and the synthesized $Cu_2(OH)_3NO_3$/ZnO samples with varying Cu:Zn mole ratios are shown in Fig. 1a. The diffraction peak at ~13° corresponds to the basal distance (6.96 Å) typically reported for the $Cu_2(OH)_3NO_3$ layered materials [26,27,29,36]. It was observed that the $Cu_2(OH)_3NO_3$/ZnO derived from the Cu:Zn molar ratio = 2:1 contains two crystalline phases, monoclinic $Cu_2(OH)_3NO_3$ (JCPDF card no. 74-1749) and hexagonal ZnO (JCPDF card no. 36145). However, with the increased Cu:Zn molar ratios to 4:1 and 6:1, the structural characteristics of $Cu_2(OH)_3NO_3$ becomes more evident, whereas the diffraction peaks corresponding to the ZnO phase (at 34.4° and 47.4°) become weaker in intensity. This is possibly due to a full coverage of $Cu_2(OH)_3NO_3$ layers on the ZnO particles. The sharp and well-defined peaks reflected high degree of crystallinity for all synthesized samples. No diffraction peaks corresponding to neither $Zn(OH)_2$, CuO nor $Cu(OH)_2$ phases were observed. It should be pointed out that, to our knowledge, this metal oxide assisted route to synthesize copper hydroxide nitrate has never been reported. The conversion of copper nitrate to copper hydroxyl nitrate possibly resulted from the availability of hydroxyl groups on the ZnO solid base. In a previous study, the basic strength of a ZnO sample was reported as $7.2 < H < 9.3$ in an Hammett indicator scale, indicating a fairly high strength comparing with those of ZrO_2, TiO_2, CaO and SrO [37].

From Fig. 1b, IR measurements also confirm the formation of copper hydroxide nitrate in the system studied. In a good agreement with previously reported works [26–29] the IR peaks at 876, 785 and 676 cm^{-1} can be assigned to hydrogen bonding frequencies related to Cu—O—H. The peaks at 1048 (ν_1), 810 (ν_2), 1340, 1348 and 1429 cm^{-1} (ν_3) can be attributed to the vibration modes of NO_3^- ions [27]. The symmetric and asymmetric stretching modes of NO_3^- at 1429 and 1340 cm^{-1} suggested the presence of NO_3^- between copper hydroxide layers. The IR band at 1048 cm^{-1} corresponds to the N—O stretching vibration of a monodentrate O—NO groups [38],

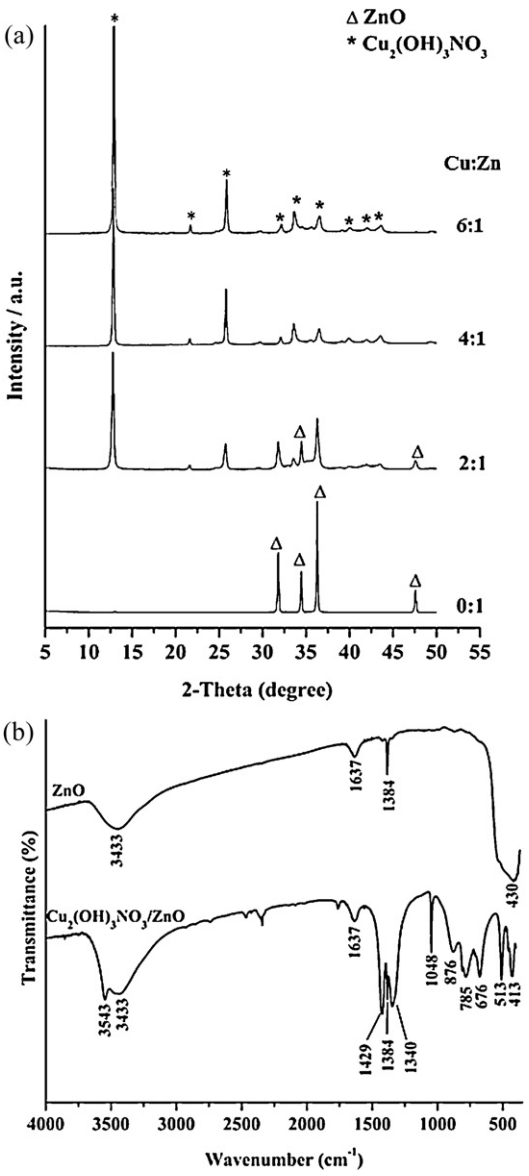

Fig. 1. (a) Powder XRD patterns of $Cu_2(OH)_3NO_3$/ZnO samples at varying the Cu:Zn molar ratios in comparison to that of ZnO and (b) Infrared spectra of $Cu_2(OH)_3NO_3$/ZnO (Cu:Zn = 4:1) and ZnO powder.

whereas the band at 1637 cm^{-1} can be ascribed to a HOH bending mode. The peaks at 3543 cm^{-1} and 3433 cm^{-1} indicated more than one type of hydroxyl groups in the structure [27,29]. Note that the characteristic peak of ZnO at 430 wavenumber [39] was not clearly observed in the $Cu_2(OH)_3NO_3$/ZnO (Cu:Zn = 4:1) sample, possibly due to signal overlapping and the full coverage of $Cu_2(OH)_3NO_3$ layers formed on the ZnO particles as previously discussed.

Noticed from Fig. 2a, the microcrystalline ZnO substrate resembles to a bunch of double flowers. Although the $Cu_2(OH)_3NO_3$/ZnO composites did not retain the flower-like microstructure of their substrate (Fig. 2b–d) a resemblance of aggregates of flake-like plates (~400 nm in thickness) morphology can be still observed. X-ray fluorescence (XRF) was employed to perform elemental analysis in the composite samples, and the results were included in Table 1. The XRF results suggest that the content of Cu was found to increase in the composites with increased Cu:Zn molar ratios. This finding was consistent with the results from EDX microanalyses, Fig. 3, revealing the presence of Cu and Zn on the composite surface, and that the content of Cu was found to be higher in the composites

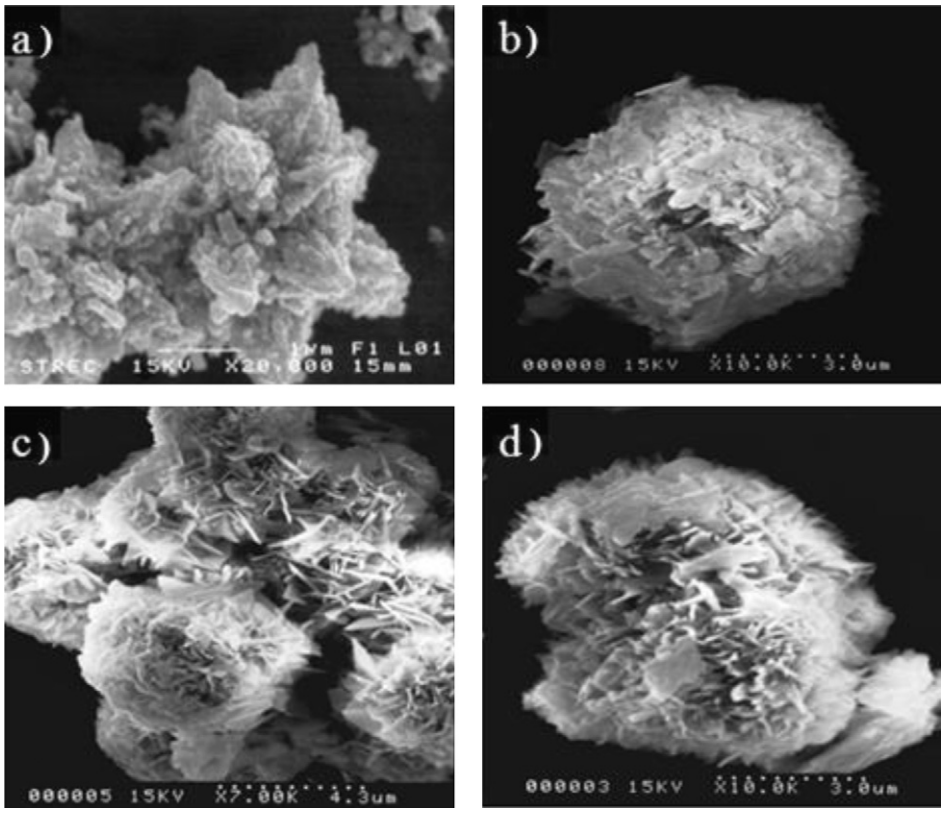

Fig. 2. SEM images of the flower-like ZnO (a) and (b–d) $Cu_2(OH)_3NO_3$/ZnO at the Cu:Zn molar ratios of 2:1, 4:1 and 6:1, respectively.

Table 1
Elemental concentration in the $Cu_2(OH)_3NO_3$/ZnO samples at various Cu:Zn molar ratios obtained by XRF analysis.

Cu:Zn	Concentration (wt%)		Depth of penetration (μm)
	Cu	Zn	
2:1	47.97 ± 0.048	15.09 ± 0.014	0.13–0.16
4:1	49.86 ± 0.048	11.30 ± 0.012	0.14–0.17
6:1	60.09 ± 0.054	1.59 ± 0.004	0.13–0.16

derived from the higher Cu:Zn. However, as shown in Table 2, the Cu:Zn ratios vary in different areas of the sample surface, suggesting that the Cu-containing compound does not homogeneously incorporated with the ZnO particles.

3.2. Catalytic activity of $Cu_2(OH)_3NO_3$/ZnO

The performance in decolorization of 500 ppm aqueous methyl orange (MO) solution over the $Cu_2(OH)_3NO_3$/ZnO composites at varying Cu:Zn ratios were examined over a period of time as shown in Fig. 4a. Notably, the color removal efficiencies reached 99% within 1.5 min of the treatments by all composites at 25 °C under atmospheric pressure (Fig. 4a). It was noticed from Fig. 4a and b, that the $Cu_2(OH)_3NO_3$/ZnO composites prepared with relatively high Cu:Zn molar ratios oxidized MO slightly faster than the samples having lower Cu content, implying that the amount of copper may play a crucial part to the reaction kinetics of MO degradation. Determined using first-order kinetic model, it was found that the higher rate constants for the catalytic wet oxidation of MO were obtained from the $Cu_2(OH)_3NO_3$/ZnO with the higher Cu:Zn molar ratios (6:1, 4.4 min^{-1}; 4:1, 3.9 min^{-1}; 2:1, 3.6 min^{-1}). The first order kinetic plot in Fig. 4b was focused in the range of shorter reaction time, because after 1.5 min the color removal efficiencies reached 99%. Statistical analyses suggested that the kinetic constants for the MO decoloriaztion by each catalyst (2:1, 4:1 and 6:1) are significantly different due to the Cu:Zn molar ratios at the level of $p < 0.05$. Fig. 4c shows a characteristic absorption band at 464 nm corresponding to a conjugated azo bond structure in the MO molecule [40]. In this work, the absorption band at 464 nm become weaker in intensity after treatment with $Cu_2(OH)_3NO_3$/ZnO composites. Therefore, in consistent with the result in Fig. 4b, the UV–vis spectra of MO after 1-min treatments over the composites at varying ratios indicate that the composites with higher Cu: Zn molar ratios lead to the higher color removal rates.

Chemical oxygen demand (COD) and total organic carbon (TOC) values are generally determined to examine the water quality. According to the results (Fig. 5) COD removal efficiencies over the

Table 2
EDX analysis in different areas of the $Cu_2(OH)_3NO_3$/ZnO samples at various Cu:Zn molar ratios.

Cu:Zn	% Element								
	Area #1			Area #2			Area #3		
	Cu	Zn	O	Cu	Zn	O	Cu	Zn	O
2:1	25.74	14.80	59.46	39.85	5.52	54.63	23.52	26.30	50.18
4:1	37.78	5.10	57.11	45.08	1.90	53.01	54.09	2.82	43.08
6:1	53.70	3.40	42.90	48.12	1.48	50.40	35.73	1.32	62.95

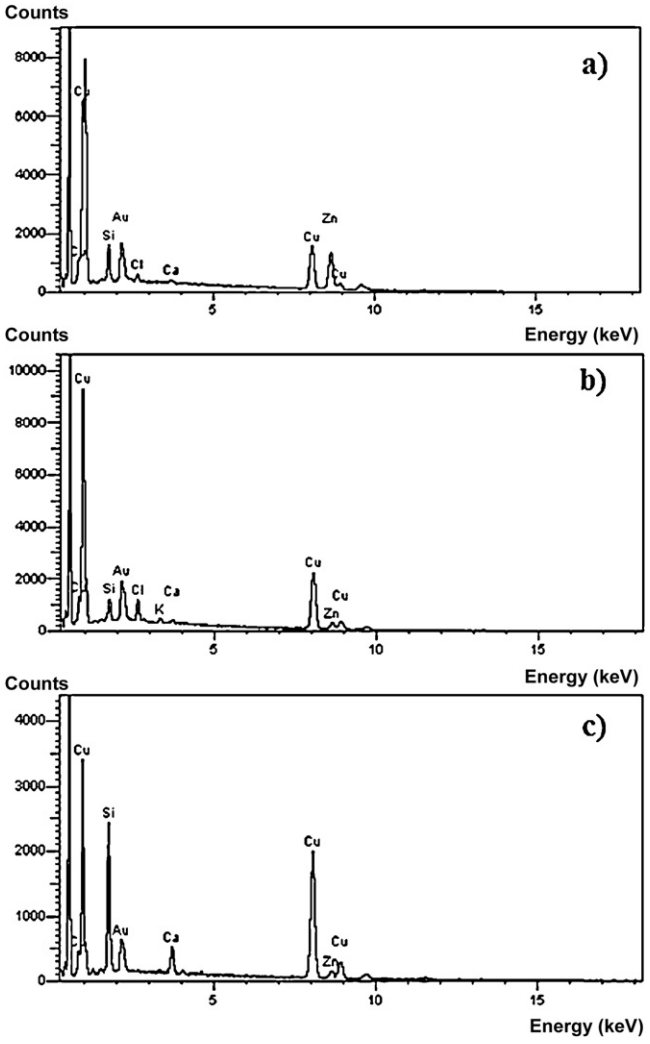

Fig. 3. EDX analysis of the $Cu_2(OH)_3NO_3$/ZnO samples at various Cu:Zn molar ratios (a) 2:1, (b) 4:1 and (c) 6:1, respectively.

catalyst are about 88% and 98% after treatment for 5 and 20 min, respectively. In addition, the results in Fig. 5 also suggest organic carbon mineralization and CO_2 evolution from the oxidation of MO after 5- and 20-min of the treatments by $Cu_2(OH)_3NO_3$/ZnO (Cu:Zn = 4:1) resulting in 84%, and 94% TOC removal efficiencies, respectively. Thus, at this catalyst loading condition, the effective decolorization of MO occurred through the fragmentation of the dye into some other colorless compounds, as well as, the mineralization of MO.

3.3. Possible mechanism and degradation pathway

The BET surface area of catalysts prepared by the Cu:Zn molar ratios of 2:1, 4:1, 6:1 are 10.81, 8.85, and 5.76 m^2/g, respectively. From Fig. 4a, the $Cu_2(OH)_3NO_3$/ZnO with lower specific surface area gave the higher color removal efficiency, suggesting that the effective color removal was not due to adsorption of dye onto the solid surface. It was found that the higher performance catalysts have lower surface areas, and thus the MO degradation rates are not proportional to the BET surface area of the catalyst. This maybe because copper hydroxyl nitrate deposited on the surface and filled in the pores of the ZnO, resulting in the materials with lower surface areas. It should be also pointed out that the lower surface area materials also have reduced pore volumes, as the pore volumes of catalysts prepared by the Cu:Zn molar

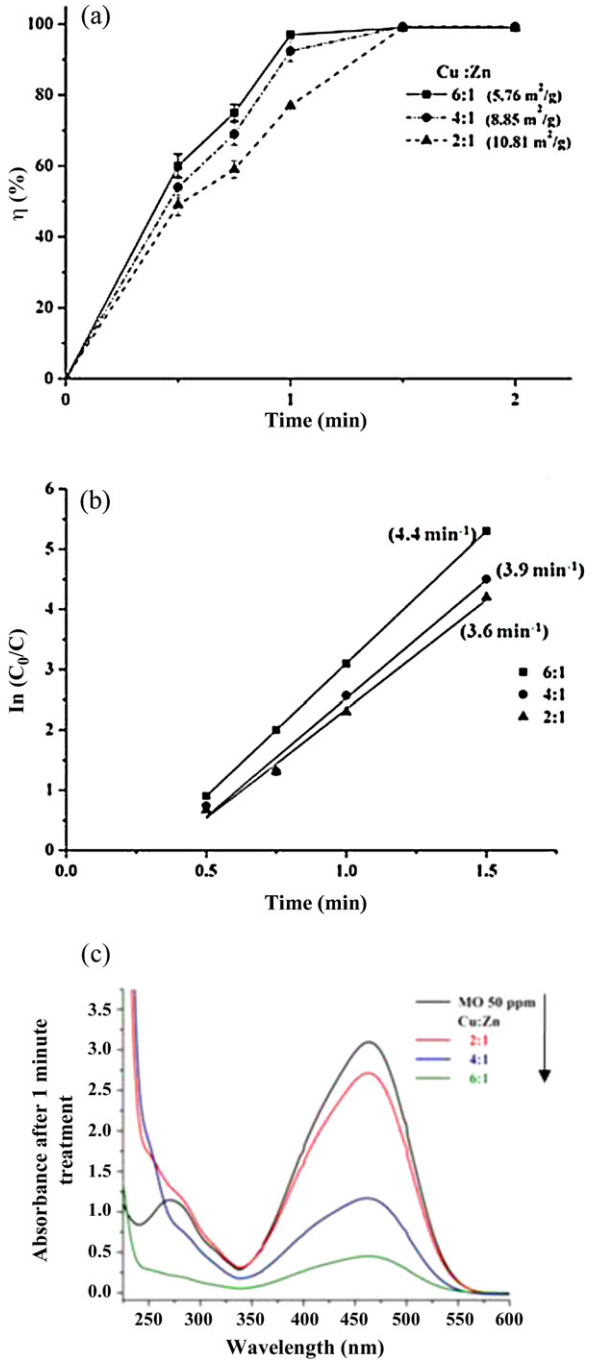

Fig. 4. (a) Color removal efficiency upon time using $Cu_2(OH)_3NO_3$/ZnO catalysts as a function of Cu:Zn molar ratio and surface area (m^2/g), (b) kinetic of methyl orange oxidation catalyzed by $Cu_2(OH)_3NO_3$/ZnO as a function of Cu dosage and (c) UV–vis absorption spectrum of fresh MO (50 ppm) and those of oxidized MO after 1-min treatment by the catalysts with various Cu:Zn molar ratiosunder ambient conditions. Initial concentration of MO = 500 ppm; catalyst loading = 3 g L^{-1}.

ratios of 2:1, 4:1, 6:1 are 0.08, 0.07, and 0.02 cc/g, respectively. In addition, approximately the same color removal efficiency (~99%) was also observed when a dispersion of $Cu_2(OH)_3NO_3$/ZnO (Cu:Zn = 4:1) in aqueous MO solution was kept in the dark under similar experimental conditions mentioned above. Thus, light had no influence to the catalytic activity of composite. As a result, one could suggest a catalytic wet oxidation (CWO) process, in which the dye undergoes aerial oxidation over the composites. Note that, commercially supplied ZnO powder can also be replaced the flower-like ZnO to produce the $Cu_2(OH)_3NO_3$/ZnO composites,

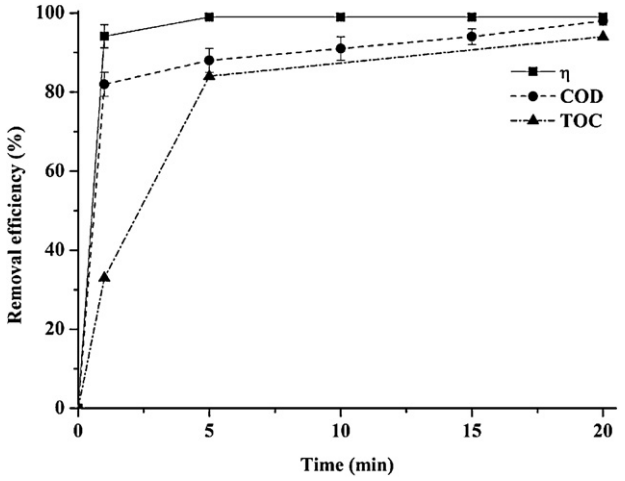

Fig. 5. Color (η), COD and TOC removal efficiencies upon treatment of MO aqueous solution by the $Cu_2(OH)_3NO_3$/ZnO (Cu:Zn = 4:1). Initial concentration of MO = 500 ppm; catalyst loading = 3 g L^{-1}.

having almost the same catalytic activity. In an attempt to understand the nature of MO degradation over the $Cu_2(OH)_3NO_3$/ZnO composites, additional MO degradation reactions were conducted in various experimental conditions and reported in Fig. 6.

It is well known that CWO catalysts require oxygen to degrade organic compounds. Accordingly, if catalytic wet oxidation (CWO) was the major process responsible for MO degradation, the oxidation rate of MO should be directly proportional to the oxygen concentration. One of the experiments was conducted under vacuum (setup Fig. S2) here the MO solution was thoroughly degassed prior to being used. As reported in Fig. 6, the color removal efficiency of MO under vacuum was about 7.72%, which is much lower than under ambient conditions (~100%). The proposed mechanism of CWO reactions outlined by Ma et al. [44] may be applied to describe the CWO reactions occurring here.

$$RH + Cu^{2+} \rightarrow R^{\bullet} + Cu^{+} + H^{+} \quad (3)$$

$$Cu^{+} + O_2 \rightarrow Cu^{2+} + O_2^{-} \quad (4)$$

$$2O_2^{-} + 2H_2O \rightarrow 2OH^{-} + H_2O_2 + O_2 \quad (5)$$

$$H_2O_2 + Cu^{2+} \rightarrow HO^{\bullet} + OH^{-} + Cu^{2+} \quad (6)$$

$$HO^{\bullet} + MO \rightarrow \text{degradationproducts} \quad (7)$$

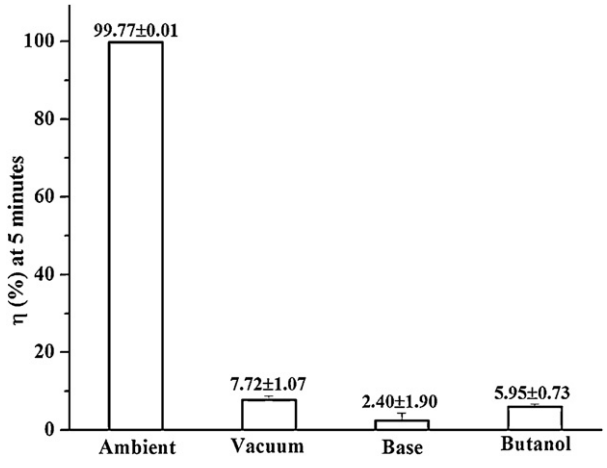

Fig. 6. Comparative results of the color removal efficiency after 5 min treatment of MO with $Cu_2(OH)_3NO_3$/ZnO (Cu:Zn = 4:1), with varying experimental conditions.

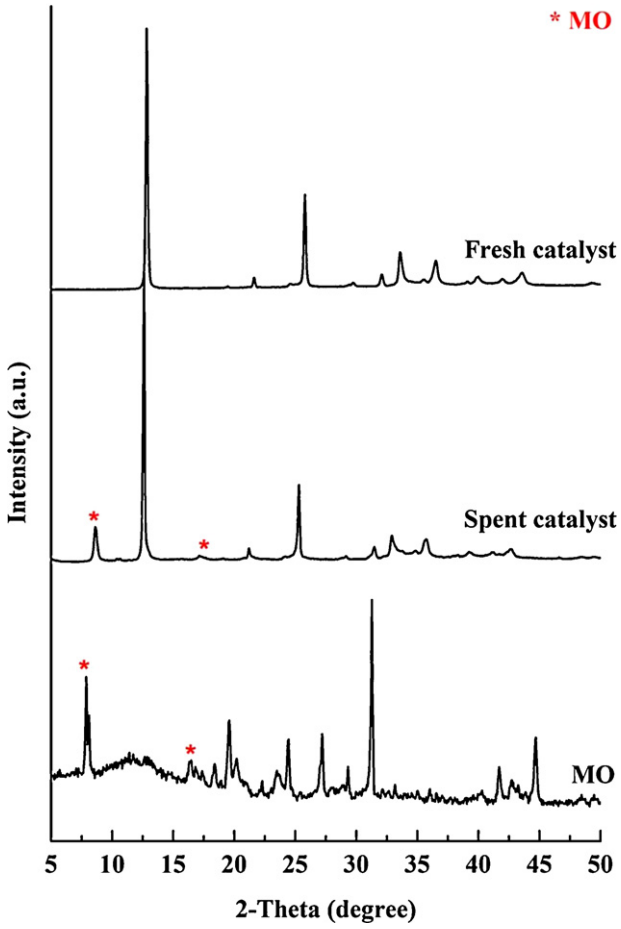

Fig. 7. Powder XRD patterns of $Cu_2(OH)_3NO_3$/ZnO samples (Cu:Zn = 4:1) before and after reaction comparing with that of MO.

From the proposed model, Cu (II) in the catalyst undergoes reduction reaction forming Cu (I) which further reacts with oxygen dissolved in an aqueous solution. Subsequently, H_2O_2 is generated as intermediates through the reaction of O_2^- and water molecules. Following this model, it is possible that hydroxyl radical is created when $Cu_2(OH)_3NO_3$ decomposed H_2O_2 intermediates. Finally, MO molecule was attacked by hydroxyl radicals. According to the proposed CWO reaction mechanism, the presence of radical scavenging reagents such as NaOH and tert-butanol, should significantly inhibit the oxidation of MO. The result in Fig. 6 represents that adding NaOH and tert-butanol gave low color removal efficiencies of 2.40% and 5.95%, respectively after 5-min treatments using $Cu_2(OH)_3NO_3$/ZnO (Cu:Zn = 4:1). These results strongly support that the decomposition of MO occurred through a radical pathway.

Previously discussed from the result in Fig. 4c, the decrease in intensity of the absorption band corresponding to MO indicated the cleavage of the azo group, and hence decolorization of the dye solution. No spectral shift corresponding to possible complexation between dye molecules and metal cations [41–43] was observed in our system. Besides this, Fig. 7 shows that the $Cu_2(OH)_3NO_3$/ZnO catalyst undergoes no significant structural change after 20 min reaction. Apart from the typical features corresponding to the $Cu_2(OH)_3NO_3$ crystalline phase, extra diffraction peaks were observed at 8.9° and 17.1° which correspond to crystallized MO on the catalyst surface. The observed slight shift in peak positions is possibly due to microstrains on the sample occurring during the drying process. According to XRD results, there is no evidence of any new crystalline phase in the used catalyst, ruling

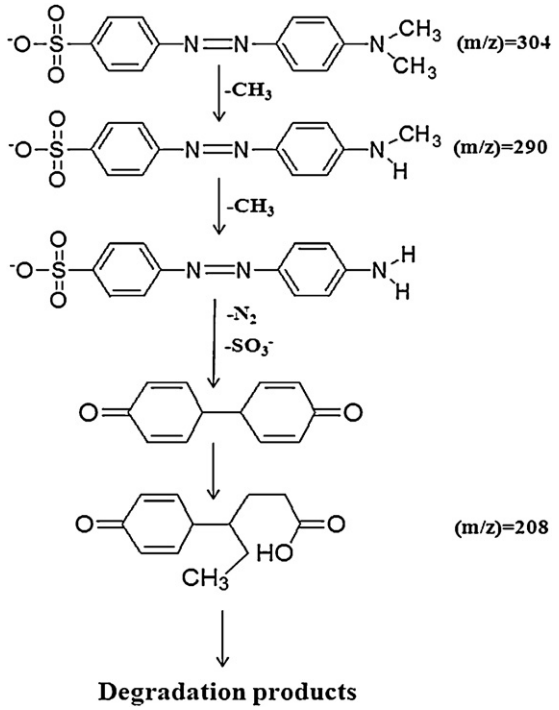

Fig. 8. Possible MO degradation pathway producing molecular fragments as detected by LC/MS.

out the possibility of complexation between the $Cu_2(OH)_3NO_3$/ZnO composite and MO. Consequently, all results discussed above support the degradation of MO over $Cu_2(OH)_3NO_3$/ZnO composites *via* a catalytic wet oxidation process. Nevertheless, in contrast to conventional CWO catalysts, $Cu_2(OH)_3NO_3$/ZnO is highly active with no requirement of air or oxygen flow or any additional oxidant.

In an attempt to determine the nature of MO degradation products, LC/MS analysis of decolorized MO solutions revealed the presence of three chemical species after a 5 min reaction period. At level of 99% decolorization, the chemical species identified were unreacted MO (M_w = 304) and two product species with m/z = 290 and 208, corresponding to MO fragments (Fig. S3). The reaction steps in wet oxidation of MO catalyzed by $Cu_2(OH)_3NO_3$/ZnO observed by LC/MS are given in Fig. 8.

3.4. Catalyst reusability

This part focuses on possibility of recovery, recyclization, and regeneration of the catalyst. By simple centrifugation and decantation, it was found that the $Cu_2(OH)_3NO_3$/ZnO (Cu:Zn = 4:1) catalyst can be reused for three consecutive runs, without any further treatment, maintaining the color removal efficiencies of 99%, and the COD and TOC removal efficiencies of greater than 90% after 20-min reaction as shown in Fig. 9a. As previously discussed, adsorption of MO on the catalyst surface occurred. However, based on the high color removal efficiencies for three cycle utilization, the presence of adsorbed MO on the surface of used catalyst did not affect the color removal efficiencies. Nevertheless, when the catalyst was further reused without treatment in the 4th run, it was found that the color removal efficiency dropped from 99% to about 37% as reported in Fig. 9b. Therefore, the used catalyst after the 3rd run requires suitable regeneration prior to further use. Possible regeneration methods include refluxing method, calcination under a suitable atmosphere, rinsing by appropriate solvent or some combinations of processes [12,19,45,46]. Due to the low thermal stability

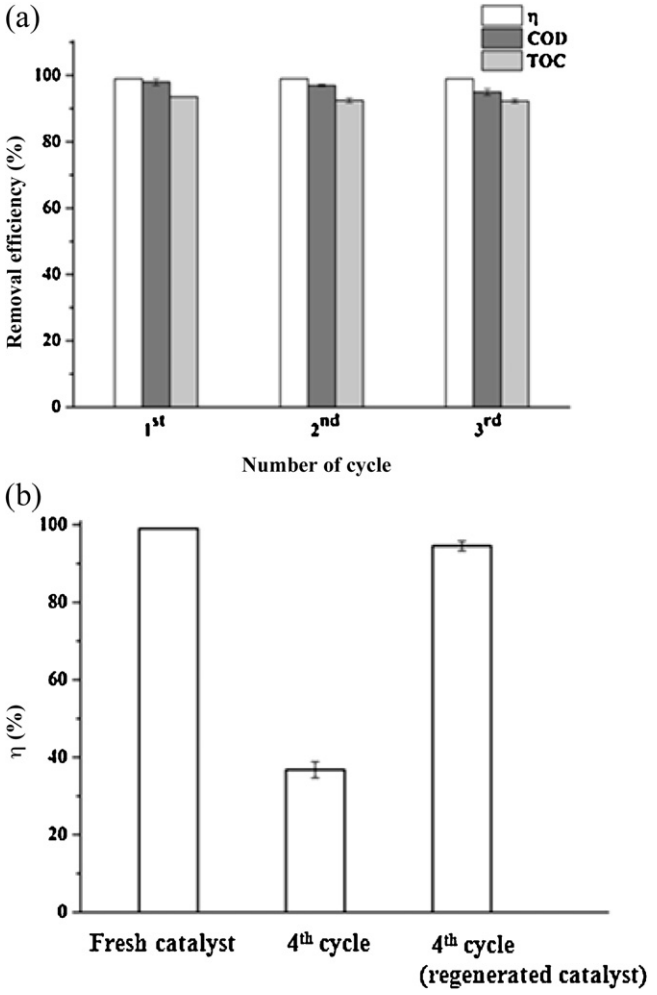

Fig. 9. (a) Color (η), COD and TOC removal efficiency for suspension of the $Cu_2(OH)_3NO_3$/ZnO (Cu:Zn = 4:1) in MO aqueous solution during consecutive runs and (b) comparative results of the color removal efficiencies (η) of MO by the $Cu_2(OH)_3NO_3$/ZnO (Cu:Zn = 4:1) in the 1st and 4th cycles without regeneration, and that of the 4th cycle obtained by employing the regenerated catalyst after the 3rd run *via* mild acid wash. Initial concentration of MO = 500 ppm; catalyst loading = 3 g L^{-1}.

of copper hydroxide nitrate and the solubility of metal oxide in acid, the spent $Cu_2(OH)_3NO_3$/ZnO was regenerated by washing with weak acid to remove the unreacted MO and, possibly, degradation products adsorbed on the catalyst surface without causing serious damages to the catalyst. It was found that, after filtration, washing the spent catalyst (from the 3rd run) with 5 mM HCl(aq) for 20 min, and rinsing with water followed by drying at 100 °C, the regenerated catalyst can be employed in the 4th cycle giving the color removal efficiency of 95% as shown in Fig. 9b. This color removal efficiency is lower than those obtained from the first three cycles, probably due to some loss of active copper species during acid washing.

Table 3 reports that, after 20-min MO degradation, the $Cu_2(OH)_3NO_3$/ZnO (Cu:Zn = 4:1) catalyst slightly dissolved in the dye solution giving the concentration of Cu and Zn ions of 4.3 and 0.5 ppm in the first cycle. In the subsequent cycles, the solubility of catalyst was found lower. According to the high color, COD, and TOC removal efficiencies (>90%) for three cycle utilization, this trace amount of meal leaching did not affect the removal efficiencies, implying that the $Cu_2(OH)_3NO_3$/ZnO catalyst was stable for three consecutive cycles with no requirement of catalyst regeneration (Fig. 9a). However, due to the results of metal leaching, there may be questioning of the MO degradation *via* homogeneous

Table 3
Solubility of the $Cu_2(OH)_3NO_3$/ZnO (Cu:Zn = 4:1) catalyst in MO aqueous solution after 20 min treatments in the 1st–3rd cycle utilizations.

Cycle number	Solubility of metal in the dye solution	
	Cu/ppb	Zn/ppb
1	4293.2 ± 42.1	459.5 ± 8.6
2	1398.6 ± 42.1	352.7 ± 6.5
3	506.8 ± 37.2	116.7 ± 4.7

reaction catalyzed by copper dissolved in the dye solution. From XRF and AA results (Tables 2 and 3) less than 5 ppm of copper ions was detected in the MO solution after 20-min treatment by the $Cu_2(OH)_3NO_3$/ZnO (Cu:Zn = 4:1) catalyst, which contains Cu approximately 50% by weight. As the results, one could calculate the percentage of Cu loss upon catalytic oxidation of 500 ppm MO(aq) being around 0.8 wt% of total copper content in the catalyst. An additional experiment was conducted to probe the catalytic activity of copper ions in degradation of MO through a homogeneous route. The concentration of MO was quantified after 120-min treatment of 100 ppm MO(aq) in the presence of 80 mM $CuSO_4$ (~5 ppm of Cu^{2+}) giving very low color removal efficiency of 1%. This result implies that the dissolved Cu^{2+} in the MO solution does not effectively catalyze the MO decolorization under ambient conditions, and that the homogeneous oxidation of MO (if occur) was not the main process for the MO degradation in this study.

A comparison of the oxidative efficiency and reaction conditions of our prepared catalyst with a number of reported ambient CWO catalysts is given in the Supplementary Data. Recently, reported catalysts, CuO–MoO_3–P_2O_5 and $PtHCa_2Nb_3O_{10}$, shows similarity with our system for decolorization of MO under ambient conditions, and in the absence of additional oxidant [44,47]. Notably, in the oxidation reaction of 300 ppm MO catalyzed using CuO–MoO_3–P_2O_5, only 55% color removal was achieved after 30 min with catalyst loading levels being 4.3 times higher than that required for our $Cu_2(OH)_3NO_3$/ZnO system. On the other hand, $PtHCa_2Nb_3O_{10}$ was employed as a catalyst for oxidation of 20 ppm MO in the absence of light, but the decolorization efficiency was not reported. However, UV–vis spectral changes of MO over time in this example indicated that approximately 50% MO degradation occurred after 250 min, which is far less efficient than our catalyst system. Therefore, the catalytic activity of $Cu_2(OH)_3NO_3$/ZnO to MO oxidation is far superior to that of CuO–MoO_3–P_2O_5 and $PtHCa_2Nb_3O_{10}$, with the added benefit of being more cost-effective to produce.

4. Conclusion

In summary, $Cu_2(OH)_3NO_3$/ZnO is a highly efficient CWO catalyst for MO oxidation, which is reusable and highly active under ambient conditions without the addition of other oxidants. It was possible to regenerate the deactivated catalyst by washing with weak acid giving almost the same activity compared to that of the fresh catalyst. Nevertheless, other regeneration methods may be suitable to maintain the high catalytic activity in the long run. The $Cu_2(OH)_3NO_3$/ZnO catalysts were currently under further investigations on effects of pH, temperature and variation of organic wastes on their catalytic efficiencies, and the results on these will be reported in the near future.

Acknowledgments

This work was partially supported by Center of Excellence for Innovation in Chemistry (PERCH-CIC), Office of the Higher Education Commission, and Central Instrument Facility (CIF), Faculty of Science, Mahidol University. Authors are also thankful for technical assistance from Dr. Uracha Ruktanonchai, Asst. Prof. Atitaya Siripinyanond, Ms. Weerawan Waiyawat, Ms. Kullavadee Karnorachai and Mr. Kraiwit Pakutsah. Financial support from the Thailand Research Fund through the Royal Golden Jubilee Ph.D Program (grant no. PHD/0119/2553) is also gratefully acknowledged.

Appendix A. Supplementary data

Supplementary data associated with this article can be found, in the online version, at http://dx.doi.org/10.1016/j.apcatb.2012.10.018.

References

[1] E.Z. Harrison, S.R. Oakes, M. Hysell, A. Hay, Science of the Total Environment 367 (2006) 481–497.
[2] B.M. Afzal, Journal of Midwifery and Women's Health 51 (2006) 12–18.
[3] G. Crini, Bioresource Technology 97 (2006) 1061–1085.
[4] H.-Y. Hu, X. Li, Y.-H. Wu, M. Sagehashi, A. Sakoda, Water Science and Technology 9 (2011) 199–207.
[5] S.K. Bhargava, J. Tardio, J. Prasad, K. Föger, D.B. Akolekar, S.C. Grocott, Industrial and Engineering Chemical Research 45 (2006) 1221–1258.
[6] Y.I. Matatov-Meytal, M. Sheintuch, Industrial and Engineering Chemical Research 37 (1998) 309–326.
[7] K.-H. Kim, J. S-KIhm, Journal of Hazardous Materials 186 (2011) 16–34.
[8] L. Szpyrkowicz, C. Juzzolino, S.N. Kaul, Water Research 35 (2001) 2129–2136.
[9] R.J. Stefan, R. Unterman, Annual Review of Microbiology 48 (1994) 525–557.
[10] M. Vidali, Pure and Applied Chemistry 73 (2001) 1163–1172.
[11] A. Vogelpohl, S.M. Kim, Journal of Industrial and Engineering Chemistry 1 (2004) 33–40.
[12] S. Keav, J.J. Barbier, D. Duprez, Catalysis Science and Technology 1 (2011) 342–353.
[13] L. Zhao, J. Ma, Z. Sun, H. Liu, Applied Catalysis B: Environmental 89 (2009) 326–334.
[14] R.F.F. Pontesa, J.E.F. Moraes, A. Machulek Jr., J.M. Pinto, Journal of Hazardous Materials 176 (2010) 402–413.
[15] H.R. Jafry, M.V. Liga, Q. Li, A.R. Barron, Environmental Science and Technology 45 (2011) 1563–1568.
[16] A. Mehrdad, R. Hashemzadeh, Ultrasonics Sonochemistry 17 (2010) 168–172.
[17] B.D. Witte, J. Dewulf, K. Demeestere, H.V. Langenhove, Journal of Hazardous Materials 161 (2009) 701–708.
[18] K. Ayouba, E.D.V. Hullebuschb, M. Cassirc, Alain Bermond, Journal of Hazardous Materials 178 (2010) 10–28.
[19] Y. Liu, D. Sun, Applied Catalysis B: Environmental 72 (2007) 205–211.
[20] W. Li, S. Zhao, B. Qi, Y. Du, X. Wang, M. Huo, Applied Catalysis B: Environmental 92 (2009) 333–340.
[21] Y. Zhang, D. Li, Y. Chen, X. Wang, S. Wang, Applied Catalysis B: Environmental 86 (2009) 182–189.
[22] J. Huang, X. Wang, S. Li, Applied Surface Science 257 (2010) 116–121.
[23] L.F. Liotta, M. Gruttadauria, G.D. Carlo, G. Perrini, V. Librando, Journal of Hazardous Materials 162 (2009) 588–606.
[24] Y. Zhan, H. Li, Y. Chen, Journal of Hazardous Materials 180 (2010) 481–485.
[25] Y. Zhan, X. Zhou, Bei. Fu, Y. Chen, Journal of Hazardous Materials 187 (2010) 348–354.
[26] S.H. Lee, Y.S. Her, E. Matijevic, Journal of Colloid and Interface Science 186 (1997) 193–202.
[27] C. Henrist, K. Traina, C. Hubert, G. Toussaint, A. Rulmont, R. Cloots, Journal of Crystal Growth 254 (2003) 176–187.
[28] M. Meyn, K. Beneke, C. Lagaly, Inorganic Chemistry 32 (1993) 1209–1215.
[29] H. Niu, Q. Yang, K.A. Tang, Materials Science and Engineering B 135 (2006) 172–175.
[30] A. Srikhaow, S.M. Smith, Research On Chemical Intermediates (2012), http://dx.doi.org/10 1007/s11164-012-0619-5.
[31] APHA, AWWA, WEF, Standard Method for the Examination of Water and Waste water, 19th ed., APHA, Washington, DC, 1995.
[32] V. Teeranachaideekul, E.B. Souto, V.B. Junyaprasert, R.H. Müller, European Journal of Pharmaceutics and Biopharmaceutics 67 (2007) 141–148.
[33] Z. Xu, C. Jing, F. Li, X. Meng, Environmental Science and Technology 42 (2008) 2349–2354.
[34] B. Stöffler, G. Luft, Chemical Engineering and Technology 21 (1999) 409–412.
[35] K. Okawa, K. Suzuki, T. Takeshita, K. Nakano, Journal of Hazardous Materials 127 (2005) 68–72.
[36] G.G.C. Arizaga, K.G. Satyanarayana, F. Wypych, Solid State Ionics 178 (2007) 1143–1162.
[37] S.J. Yoo, H.-S. Lee, B. Veriansyah, J.-D. Kim, Y-W.J. Kim, Lee Bioresource Technology 101 (2010) 8686–8689.
[38] K. Nakamoto, Infrared and Raman Spectroscopy of Inorganic and Coordination Compound, 4th ed., John Wiley & Sons, New York, 1986.
[39] J. Zhao, L. Zhao, X. Wang, Frontiers of Environmental Science and Engineering in China 2 (2008) 415–420.

[40] Y.-P. Chen, S.-Y. Liu, H.-Q. Yu, H. Yin, Q.-R. Li, Chemosphere 72 (2008) 532–536.
[41] Y.-H. Luo, J. Huang, J. Jin, X. Peng, W. Schmitt, I. Ichinose, Chemistry of Materials 18 (2006) 1795–1802.
[42] Y.-H. Luo, J. Huang, I. Ichinose, Journal of the American Chemical Society 127 (2005) 8296–8297.
[43] I. Ichinose, K. Kurashima, T. Kunitake, Journal of the American Chemical Society 126 (2004) 7162–7163.
[44] H. Ma, Q. Zhao, B. Wang, Environmental Science and Technology 41 (2007) 7491–7496.
[45] Y. Zheng, A.D. Jensen, J.E. Johnsson, Industrial and Engineering Chemical Research 43 (2004) 941–947.
[46] S.C. Kim, S.W. Nahm, W.G. Shim, J.W. Lee, H. Moon, Journal of Hazardous Materials 141 (2007) 305–314.
[47] E. Dvininov, U.A. Joshi, J.R. Darwent, J.B. Claridge, Z. Xu, M.J. Rosseinsky, Chemical Communications 47 (2011) 881–883.